

Silhouette-based Gait Foundation Model

Dingqiang Ye¹, Chao Fan^{2*}, Kartik Narayan¹,
Bingzhe Wu², Chengwen Luo², Jianqiang Li², and Vishal M. Patel¹

¹ Johns Hopkins University ² Shenzhen University

dye6@jh.edu, chaofan996@szu.edu.cn, knaraya4@jh.edu,

wubingzheagent@gmail.com, {chengwen, lijq}@szu.edu.cn, vpatel136@jhu.edu

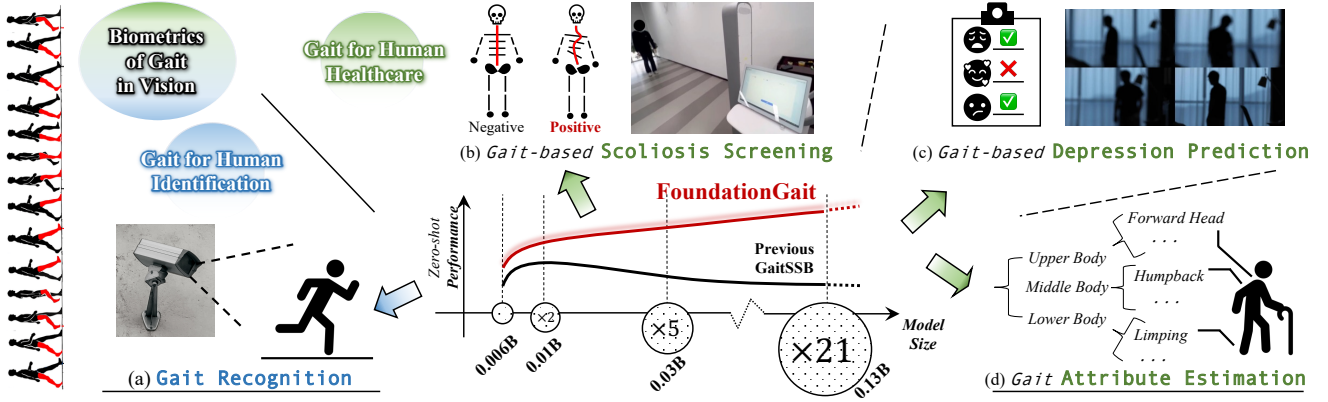


Figure 1. **FoundationGait**: A Scalable and Unified Gait Foundation Model.

Abstract

code and model: <https://github.com/ShiqiYu/OpenGait>.

Gait patterns play a critical role in human identification and healthcare analytics, yet current progress remains constrained by small, narrowly designed models that fail to scale or generalize. Building a unified gait foundation model requires addressing two longstanding barriers: (a) *Scalability* – Why have gait models historically failed to follow scaling laws? (b) *Generalization* – Can one model serve the diverse gait tasks that have traditionally been studied in isolation? We introduce **FoundationGait**, the first scalable, self-supervised pretraining framework for gait understanding. Its largest version has nearly 0.13 billion parameters and is pretrained on 12 public gait datasets comprising over 2 million walking sequences. Extensive experiments demonstrate that **FoundationGait**, with or without fine-tuning, performs robustly across a wide spectrum of gait datasets, conditions, tasks (e.g., human identification, scoliosis screening, depression prediction, and attribute estimation), and even input modality. Notably, it achieves 48.0% **zero-shot** rank-1 accuracy on the challenging in-the-wild Gait3D dataset (1,000 test subjects) and 64.5% on the largest in-the-lab OU-MVLP dataset (5,000+ test subjects), setting a new milestone in robust gait recognition. Coming

*Corresponding author.

1. Introduction

Vision-based gait offer a compelling solution for large-scale, low-cost, and non-invasive applications—including human identification and healthcare [44, 54, 55, 73, 75, 104]—as illustrated in Figure 1. Their ability to capture motion remotely and unobtrusively in unconstrained environments makes gait uniquely suitable for real-world deployment. Yet, despite this promise, a dedicated Gait Foundation Model has not emerged, even as large vision models (LVMs) [37, 57, 58] have reshaped many other domains.

Recent progress in domain-specific LVMs [18, 20, 34, 36, 68], which balance specialization with broad generalization, has demonstrated their practical value and attracted significant attention from both academia and industry [1]. Motivated by these developments, this paper takes a step toward establishing such a foundation model for gait.

Recent efforts toward building a gait foundation model generally follow two directions. The first, exemplified by BigGait [91] and subsequent studies [32, 92], focuses on transferring capacity from existing LVMs—such as DI-NOv2 [57] and Stable Diffusion [63]—into the gait domain. The second, represented by GaitSSB [12] and related

work [50, 75], instead trains gait models from scratch using vision-only or vision-language contrastive pretraining strategies [5, 61].

Both directions demonstrate that rich and discriminative gait representations can indeed be learned from walking videos under supervised or self-supervised regimes. Despite the significant progress, they—similar to much of the longstanding gait literature [15, 44, 75, 104]—remain task-specific, typically optimizing models for individual datasets rather than pursuing unified, scalable solutions.

Two core properties required for a true gait foundation model remain insufficiently explored. (a) **Size Scalability.** Although scaling laws [33] are a known driver of progress in modern foundation models, systematic investigations of scalability for video-based gait modeling are rare. In practice, we find that many gait-specific architectures fail to benefit from increasing parameters beyond relatively small sizes ($\approx 5\text{M}$); performance often saturates or even drops sharply as model capacity grows (Sec. 3.1). Historically, this limitation has been attributed to the simplicity of gait inputs—typically low-resolution (64×44), sparse binary silhouettes. (b) **Cross-task Generalization.** A defining feature of foundation models is their ability to transfer across diverse downstream tasks. Yet, gait research has traditionally treated recognition-oriented tasks and healthcare-oriented analyses as separate problem spaces, despite both relying on subtle, fine-grained motion dynamics.

Motivated by these gaps, we investigate the design principles of a true gait foundation model and introduce FoundationGait, a scalable self-supervised pretraining framework that generalizes effectively across a broad spectrum of gait datasets and downstream tasks. Our exploration centers on two key questions:

- *How can we scale gait models from 0.01B parameters to the 1B range?* Although classic part-based approaches [10] have fallen out of favor, we find that preserving fine-grained local body-part cues is essential for scaling. Building on this insight, we develop a novel *part-aware pretraining* strategy that enables FoundationGait to scale by $21\times$ over widely used baselines (e.g., DeepGaitV2’s $\approx 0.01\text{B}$ backbone [15]), while achieving consistent performance gains across datasets and tasks.
- *How can we build a sufficiently large gait corpus for pre-training?* We gather 12 public gait datasets spanning both recognition [12, 39, 64, 66, 71, 93, 100, 106, 107] and healthcare applications [44, 75, 104], forming **WebGait-2M**¹. This collection comprises over **2.35M walking sequences** (0.23B frames), exceeding the scale of datasets used to train models such as DINOv2 (0.14B frames).

In extensive experiments, FoundationGait delivers strong and consistent performance across both recognition

and healthcare settings. On challenging gait recognition benchmarks—Gait3D [100] and OU-MVLP [71], containing 1,000 in-the-wild and 5,000+ in-the-lab test subjects, respectively—FoundationGait achieves 48.0% and 64.5% zero-shot rank-1 accuracy, establishing new milestones for robust cross-condition recognition. In healthcare-oriented tasks, such as scoliosis screening on the Scoliosis1K dataset (1,000+ participants), FoundationGait reaches 97.0% accuracy after fine-tuning. Detailed evaluations and ablations are provided in Sec. 4.

Overall, this paper makes three major contributions:

- We demonstrate—systematically and for the first time—that gait models can benefit from *scaling laws*.
- We unify human identification and healthcare tasks within a single, scalable *gait foundation model*.
- Extensive experiments, with and without fine-tuning, verify the strong performance and broad generalization of **FoundationGait**.

2. Related Works

Walking patterns, as a fundamental and natural behavior, are widely recognized for their potential to reveal both human identity and health status [27, 29, 43, 44, 55, 104].

Gait Recognition. Gait recognition plays a crucial role in surveillance, particularly in unconstrained and long-distance scenarios. Recent research can be broadly categorized into five main areas [15]: (a) Mitigating gait-unrelated factors, such as the influence of RGB-encoded clothing and backgrounds in walking videos. Approaches in this direction include human parsing techniques [80, 101, 107], SMPL models [83, 84, 86, 100], multi-modal learning [14, 31], end-to-end training with inductive biases [32, 40, 91, 92], and the use of advanced sensors such as LiDAR [64, 65]. (b) Enhancing networks with gait-specific priors, such as spatio-temporal and local-global feature learning, combined with attention refinements [10, 21, 30, 41, 46, 59, 78, 79]. (c) Improving the learning process through novel frameworks, such as auto-encoder regression [19], generative modeling [28, 32, 48, 90], causal intervention [9, 76, 87], and contrastive learning [12, 50, 75]. (d) Addressing real-world challenges such as occlusion [22–24, 26, 88], clothing variation [39], and low-quality data [81]. (e) Developing improved loss functions for better optimization [69, 94, 98].

Anomaly Gait Detection. For instance, scoliosis, which affects 0.47%–5.2% of adolescents [38], was addressed by Zhou et al. [104] with the Scoliosis1K dataset, comprising over 1,000 adolescent patients, and the multi-task learning model ScoNet. Similarly, depression impacts 7.1% of U.S. adults annually [56]. Liu et al. [44] released a video-based depression dataset with 100+ participants and evaluated various gait recognition models on it. Wang et al. [75] developed a gait attribute benchmark involving 15 attributes (e.g.,

¹We do not process nor redistribute any data; “WebGait-2M” is solely a convenient name.

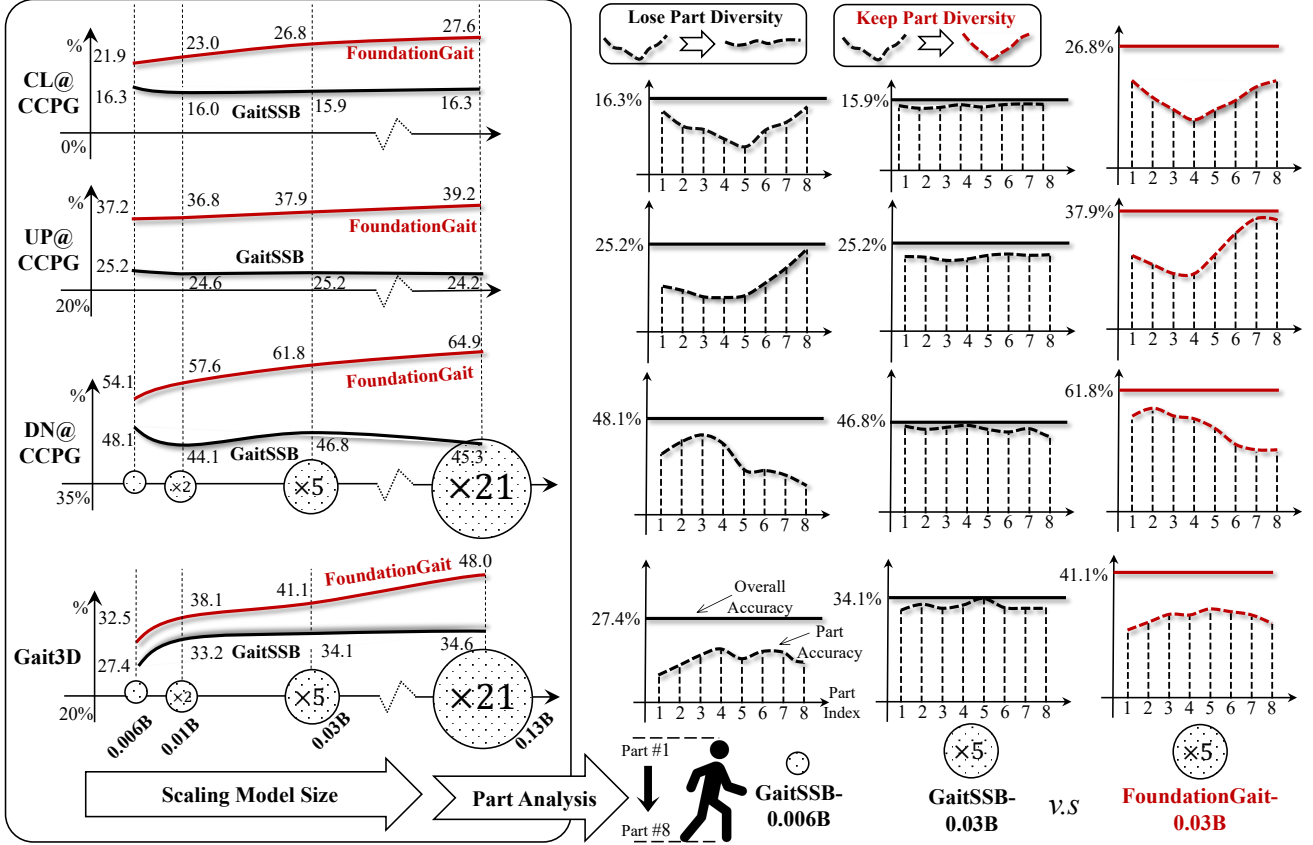


Figure 2. **Unscalable Issue** on the Self-supervised GaitSSB [12]. All models are pretrained on WebGait-2M.

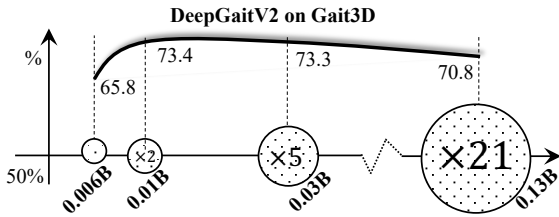


Figure 3. **Unscalable Issue** on the Supervised DeepGaitV2 [15].

toe-out, head forward, humpback) from 533 subjects and over 120,000 sequences. They also created a CLIP-like [61] model for potential use in security and healthcare.

As noted, gait analysis [82, 85] for both identification and healthcare sometimes benefits from each other. For example, Zhou [104] incorporated identification signals to enhance scoliosis classification, while Wang et al. [75] considered the potential of motion attribute estimation for identification tasks. Despite sharing a common focus on human gait, no framework has yet integrated gait recognition and anomaly detection across diverse tasks. Our FoundationGait addresses this gap, enabling a scalable and unified solution that leverages the power of large-scale pretraining.

Domain-specific Foundation Models. Beyond general-purpose LVMs [5, 37, 57, 89], domain-specific LVMs offer

a more practical solution, as they are better suited to understand field data, particularly when it differs significantly from everyday internet frames, such as satellite or industrial images [18, 20]. In related research, Khiroudkar et al. [34] introduced a comprehensive foundation model tailored for human-centric vision tasks, including 2D pose estimation, part segmentation, depth estimation, and normal prediction. Similarly, Kim et al. [36] developed a foundation model focused on human face [6, 35, 49, 51–53, 62, 103, 105] and body recognition [70]. In this paper, FoundationGait takes a step further by focusing on human gait for both recognition and healthcare applications.

3. Method

Why has the gait community yet to benefit from scaling laws? Sec. 3.1 analyzes this question, while Sec. 3.2 presents our proposed solution. For clarity, experimental settings are deferred to Sec. 4.

3.1. Scaling Issue in Gait Models

Large size is often considered a defining characteristic of foundation models [33]. However, existing representative gait models remain relatively small, typically containing fewer than 5M parameters [3, 13]. To explore the potential

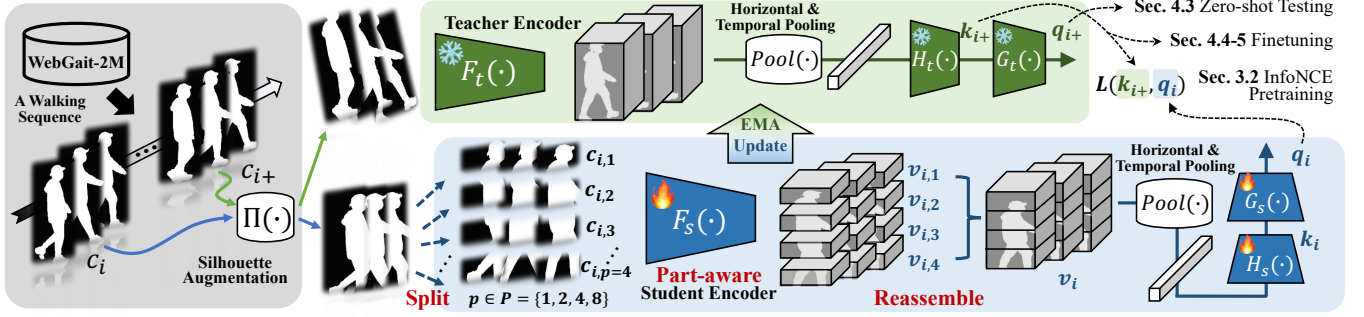


Figure 4. Overview of FoundationGait. A scalable self-supervised gait learning framework.

of scaling in this domain, we first enlarge the model size.

Scaling the Supervised DeepGaitV2. As shown in Fig. 3, when scaling up DeepGaitV2 [11, 15] on the Gait3D dataset [100], one of the largest and most challenging gait recognition benchmarks (6K+ seq.), the rank-1 accuracy quickly saturates and even degrades as model size increases.

Scaling the Self-supervised GaitSSB. We further scale up GaitSSB [12], a representative self-supervised gait pretraining framework, on the large-scale WebGait-2M dataset. Despite extensive pretraining, as shown in Fig. 2 (left, black curve), the rank-1 accuracy also saturates and even degrades on the CCPG [39] (8K+ seq. with diverse clothing variations, i.e., CL, UP, and DN) and Gait3D [100] datasets.

In contrast, our FoundationGait (red curve in Fig. 2, left) largely adheres to the expected scaling law. We find that the **devil lies in the details, specifically, in the parts**.

The gait community generally agrees that walking patterns require fine-grained descriptions. Most popular gait models [15] therefore adopt a part-based design, dividing the output feature map horizontally into several segments, each assumed to correspond to a specific body region. Under this framework, we observe that, as shown in Fig. 2 (right), **naively enlarging model size leads to diminished diversity among part features** (GaitSSB-0.006B vs. GaitSSB-0.03B), whereas **maintaining part diversity yields substantial performance gains** (GaitSSB-0.03B vs. FoundationGait-0.03B).

Intuitively, simply stacking more layers on a well-trained shallow network tends to amplify the most discriminative part features from earlier layers[2, 95]. This overemphasis easily suppresses subtle local cues and reduces feature diversity, ultimately weakening fine-grained gait representation. We therefore posit that preserving diversity among part features is the key to scaling up gait models effectively, which serves as the core motivation behind FoundationGait.

3.2. FoundationGait

As shown in Fig. 4, two non-overlap clips (\$c_i\$ and \$c_{i+}\$) are sampled from a sequence as two augmented views of identical walking patterns, where \$i \in \{1, \dots, N\}\$. Each batch con-

Algorithm 1 Pseudocode of FoundationGait Framework.

```
# F_t, H_t, G_t: teacher encoder, projector, predictor
# F_s, H_s, G_s: student encoder, projector, predictor
# P=[1,2,4,8]: part-aware hyperparameter;

for seq in loader:
    c_t, c_s = sample_two_non_overlapping_clips(seq)
    c_t, c_s = aug(c_t), aug(c_s) # two random views
    # ----- Teacher Branch -----
    with torch.no_grad():
        v_t = F_t(c_t) # (N,C,S,H,W)
        k_t = H_t(Pool(v_t)) # (N,C1,C2)
        q_t = G_t(k_t) # (N,C1,C2), zero-shot feature
    # ----- Student Branch -----
    feats = []
    # (N,...) -> len(P)*(n,...)
    subs = split_batch(c_s, len(P))
    # process each sub-batch with p in P
    for clip, p in zip(subs, P):
        # (n,C,S,H,W) -> (n*p,C,S,H//p,W)
        parts = Split(clip, p)
        # extract part-level feature maps
        f_part = F_s(parts)
        # (n*p,C,S,H//p,W) -> (n,C,S,H,W)
        f_clip = Reassemble(f_part)
        feats.append(f_clip)
    v_s = Concat(feats) # len(P)*(n,...)->(N,...)
    q_s = G_s(H_s(Pool(v_s))) # (N,C1,C2)
    # ----- Optimization -----
    loss = InfoNCE(q_s, k_t)
    loss.backward(); optimizer.step()
    T = (F_t, H_t, G_t); S = (F_s, H_s, G_s)
    MomentumUpdate(T, S) # update teacher by EMA
```

tains \$2N\$ clips forming \$N\$ positive pairs. All clips are randomly augmented by \$\Pi(\cdot)\$. Following prior self-supervised works [12, 17], one clip \$c_{i+}\$ is encoded by the teacher network to produce a projected feature \$k_{i+}\$ for downstream tasks and a predicted feature \$q_{i+}\$ for zero-shot test:

$$k_{i+} = H_t(\text{Pool}(F_t(\Pi(c_{i+})))), \quad q_{i+} = G_t(k_{i+}), \quad (1)$$

where \$F_t\$, \$H_t\$, and \$G_t\$ are the teacher's encoder, projector, and predictor, and \$\text{Pool}(\cdot)\$ is spatiotemporal aggregation [15]. See **Supplementary Materials** for details.

To encourage fine-grained part-level description, we introduce a part-aware training strategy in the student. Inspired by GaitPart [10], the other clip \$c_i\$ is first horizontally divided into \$p\$ parts (with \$p = 4\$ in Fig. 4 for simplicity), producing \$\{c_{i,j}\}_{j=1}^p\$. Then, each part is independently fed into the student encoder \$F_s\$ to obtain part feature maps \$\{v_{i,j}\}_{j=1}^p\$. These detail-enriched tensors are then reassem-

Table 1. **Overview of WebGait-2M.** It is built from twelve public train sets, treating each sequence as an individual ID in the unsupervised setting. NM, BG, CL, UP, and DN denote normal, bag-, clothing-, ups-, and pants-changing.

| Datasets | Type | Scene | Condition | Train Set | | Test Set | | Frames |
|-------------------|--------------|-------------|-----------------|-----------|-----------|----------|---------|-------------|
| | | | | #IDs | #Seq | #IDs | #Seq | |
| CASIA-B [93] | Recognition | in-the-lab | NM, BG, CL | 74 | 8,107 | 50 | 5,500 | 1,117,083 |
| CCPG [39] | Recognition | in-the-lab | CL, UP, DN, BG | 100 | 8,187 | 100 | 8,178 | 1,753,431 |
| CASIA-E [66] | Recognition | in-the-lab | NM, BG, CL | 200 | 152,697 | 814 | 626,055 | 95,581,249 |
| OUMVLP [71] | Recognition | in-the-lab | NM | 5,153 | 133,531 | 5,154 | 133,857 | 18,814,160 |
| SUSTech1K [64] | Recognition | in-the-lab | diverse | 250 | 6011 | 800 | 19,228 | 763,416 |
| CCGR [107] | Recognition | in-the-lab | diverse | 571 | 908,322 | 399 | 672,295 | 150,632,991 |
| Gait3D [100] | Recognition | in-the-wild | diverse | 3,000 | 18,940 | 1,000 | 6,369 | 3,279,239 |
| GREW [106] | Recognition | in-the-wild | diverse | 20,000 | 102,887 | 6,000 | 24,000 | 13,946,946 |
| D-Gait [44] | Healthcare | in-the-lab | Depression | 194 | 18,081 | 98 | 9,039 | 2,857,343 |
| RA-GAR [75] | Healthcare | in-the-lab | Gait Attributes | 250 | 57,155 | 283 | 65,912 | 21,304,199 |
| Scoliosis1K [104] | Healthcare | in-the-lab | Scoliosis | 745 | 745 | 748 | 748 | 447,900 |
| GaitLU-1M [12] | Unsupervised | in-the-wild | diverse | 943,884 | 943,884 | - | - | 87,235,933 |
| WebGait-2M | Unsupervised | mixed | diverse | 2,358,547 | 2,358,547 | - | - | 231,675,844 |

bled back into a unified global representation v_i , that is,

$$\begin{aligned} \{v_{i,j}\}_{j=1}^p &= F_s(\text{Split}(\Pi(c_i))), \\ v_i &= \text{Concat}(\{v_{i,j}\}_{j=1}^p). \end{aligned} \quad (2)$$

When $p=1$, no split is applied, while larger p yields finer local granularity. To balance local diversity and global consistency, a hyperparameter P (e.g., $p \in P = \{1, 2, 4, 8\}$) is used during training, where N clips are divided into $\text{len}(P)$ subsets, each with its own p . A shift-window operation, similar with SwinViT [45], is also applied to half of the samples in $\text{Split}(\cdot)$ to enhance local variation. In brief, the global feature map v_i is constructed from multiple distinct local ones, **naturally inheriting their part-level diversity**.

Finally, we compute the InfoNCE loss [25] between the student’s predictor features $q_i = G_s(H_s(\text{Pool}(v_i)))$ and teacher’s projected output k_{i+} , formulated as:

$$L(k_{i+}, q_i) = -\log \frac{\exp(\text{sim}(k_{i+}, q_i)/\tau)}{\sum_{j=1}^N \exp(\text{sim}(k_{i+}, q_j)/\tau)}, \quad (3)$$

where $\text{sim}(\cdot)$ denotes cosine similarity, $\tau = 16$ is the temperature, and $j \neq i$ indexes negative sample pairs. The pre-training scheme’s details are presented in Alg. 1. For downstream tasks, the teacher model is fine-tuned with its predictor replaced by a new task head; the part-aware training method keeps active for maintaining local diversity. See **Supplementary Materials** for details.

4. Experiments

4.1. Datasets

Pretraining Datasets. As shown in Tab. 1, we construct WebGait-2M, a large-scale gait database for pretraining, by integrating 12 public datasets spanning both human identification [12, 39, 64, 66, 71, 93, 100, 106, 107] and healthcare domains [44, 75, 104]. Consisting of 2.35M seq. and 0.23B frames, it spans an abundant range of scenes, subjects, motion patterns, clothing styles, viewpoints, and gait attributes, playing a key role in training gait foundation models.

Recognition Datasets. After pretraining, we evaluate the

Table 2. **FoundationGait Configuration.** Mapping is the projector and predictor. FLOPs are computed on a 64×44 silhouette.

| Model | Layer Depth | Parameter Size | | | Flops |
|--------|----------------|----------------|---------|--------|--------|
| | | Backbone | Mapping | Total | |
| 0.006B | (1, 1, 1, 1) | 5.9M | 32.6M | 38.5M | 1.42G |
| 0.01B | (1, 4, 4, 1) | 11.1M | 32.6M | 43.7M | 2.88G |
| 0.03B | (1, 4, 8, 4) | 33.1M | 32.6M | 65.7M | 6.76G |
| 0.13B | (1, 4, 32, 16) | 132.3M | 32.6M | 164.9M | 24.21G |

zero-shot capability on six popular gait datasets, including four in-the-lab datasets (CASIA-B [93], OUMVLP [71], CCPG [39] and SUSTech1K [64]) and two in-the-wild datasets (Gait3D [100] and GREW [106]). In fine-tuning tasks, experiments are conducted on three representative and challenging datasets: CCPG [39], offering the richest clothing diversity (coats, trousers, backpacks, and full-body outfits); Gait3D [100], targeting real-world pedestrian recognition in complex supermarket scenes with frequent occlusions and dynamic motions; and CCGR-MINI [107], a compact subset of CCGR that preserves its testing difficulty and variations in viewpoints, speeds, and terrains.

Healthcare Datasets. In healthcare, three gait-based medical datasets are used: Scoliosis1K [104], a large-scale adolescent gait dataset for non-invasive scoliosis screening in real-world settings; D-Gait [44], designed for depression risk recognition, capturing diverse views and appearances under varying walking conditions; and RA-GAR [75], a richly annotated dataset with 15 gait attributes, *i.e.*, gender, age, forward head, humpback, and limping.

4.2. Implementation Details

Protocols. Silhouettes are size-normalized following [13], resized to 64×44 , and augmented following [12]. All experiments strictly follow the official protocols.

Network. FoundationGait uses the popular DeepGaitV2’s backbone [15] as its encoder, scaled up by stacking layers. See Tab. 2 for exact model size and computation costs.

Pretraining. SGD is used with an initial learning rate of 0.05, momentum 0.9, and weight decay 5×10^{-4} . The

Table 3. **Zero-shot Performance Comparison.** Yellow regions indicate within-domain evaluations, others are cross-domain.

| Mode | Source Dataset | Method | Target Dataset | | | | | | | | | | | |
|---------------------|----------------|----------------------|----------------|------|------|--------------|--------------|--------|------------|-----------|------|------|------|----------------|
| | | | CASIA-B [93] | | | OU-MVLP [71] | Gait3D [100] | | GREW [106] | CCPG [39] | | | | SUSTech1K [64] |
| | | | NM | BG | CL | Rank-1 | Rank-1 | Rank-5 | Rank-1 | CL | UP | DN | BG | Rank-1 |
| Supervised Training | CASIA-B | GaitSet [3] | 95.8 | 90.0 | 75.4 | 9.6 | 6.5 | 14.4 | 9.4 | 9.1 | 14.8 | 15.5 | 23.8 | 12.7 |
| | | GaitPart [10] | 96.1 | 90.7 | 78.7 | 10.8 | 6.1 | 13.1 | 9.3 | 10.4 | 15.4 | 16.1 | 20.6 | 13.4 |
| | | DeepGaitV2 [15] | 93.8 | 87.1 | 61.3 | 15.2 | 12.1 | 23.4 | 15.0 | 11.9 | 21.0 | 21.8 | 35.8 | 24.4 |
| | OU-MVLP | GaitSet [3] | 74.1 | 55.5 | 16.4 | 87.2 | 13.7 | 23.4 | 12.3 | 10.9 | 19.0 | 31.3 | 47.9 | 24.4 |
| | | GaitPart [10] | 73.9 | 56.9 | 20.7 | 88.6 | 11.0 | 21.9 | 14.8 | 13.3 | 20.8 | 37.5 | 47.9 | 23.2 |
| | | DeepGaitV2 [15] | 91.7 | 78.6 | 34.7 | 91.7 | 28.5 | 44.6 | 33.5 | 19.7 | 33.0 | 58.2 | 76.8 | 40.1 |
| | Gait3D | GaitSet [3] | 66.6 | 48.7 | 12.8 | 22.9 | 40.5 | 60.0 | 19.2 | 9.4 | 17.4 | 28.8 | 54.6 | 27.8 |
| | | GaitPart [10] | 61.8 | 47.0 | 13.7 | 20.3 | 22.9 | 41.3 | 14.2 | 9.0 | 16.6 | 23.6 | 42.8 | 21.4 |
| | | DeepGaitV2 [15] | 81.7 | 68.8 | 15.2 | 46.4 | 73.4 | 87.2 | 35.7 | 13.8 | 27.0 | 46.2 | 81.2 | 50.6 |
| | GREW | GaitSet [3] | 66.0 | 45.8 | 19.8 | 22.1 | 17.8 | 31.6 | 47.9 | 7.9 | 19.0 | 22.3 | 41.5 | 19.8 |
| | | GaitPart [10] | 69.2 | 52.1 | 25.4 | 25.4 | 14.1 | 25.8 | 47.6 | 7.6 | 16.2 | 17.7 | 31.2 | 18.8 |
| | | DeepGaitV2 [15] | 77.1 | 56.3 | 30.2 | 31.3 | 33.1 | 49.1 | 77.8 | 13.3 | 30.6 | 28.9 | 61.9 | 27.7 |
| Self-Supervised | GaitLU-1M | GaitSSB [12] | 83.8 | 75.7 | 28.7 | 37.2 | 24.8 | 38.0 | 16.6 | 11.3 | 20.0 | 32.5 | 50.6 | 50.3 |
| | | GaitSSB | 88.9 | 74.8 | 33.5 | 44.4 | 27.4 | 43.3 | 21.5 | 16.3 | 25.2 | 48.1 | 57.6 | 38.5 |
| | WebGait-2M | GaitSSB-0.03B | 84.2 | 64.8 | 26.0 | 39.2 | 33.2 | 51.2 | 24.7 | 16.0 | 24.6 | 44.1 | 64.9 | 41.1 |
| | | GaitSSB-0.13B | 82.8 | 64.6 | 25.9 | 38.9 | 34.6 | 53.2 | 23.0 | 16.3 | 24.2 | 45.3 | 65.9 | 36.9 |
| | | FoundationGait-0.03B | 92.0 | 72.9 | 39.4 | 57.0 | 41.1 | 59.0 | 29.1 | 26.8 | 37.9 | 61.8 | 77.1 | 48.1 |
| | | FoundationGait-0.13B | 94.0 | 75.4 | 40.2 | 64.5 | 48.0 | 66.5 | 29.4 | 27.6 | 39.2 | 64.9 | 80.8 | 49.0 |

0.13B model is trained for 80K iterations with a cosine annealing scheduler ($T_{max} = 80K$, $\eta_{min} = 1 \times 10^{-5}$), while the others are trained for 40K iterations using MultiStepLR (20K, 30K; $\gamma = 0.1$). The EMA momentum rises from 0.99 to 1.0 via a cosine schedule. Batch size is 512 with 16 frames per clip. In the part-aware student, $P = [1, 2, 4, 8]$.

Sampling. To balance data diversity, each batch samples from the 12 datasets with softmax-normalized probabilities proportional to $\log(\text{size})/3.0$, while *GaitLU*-1M is down-weighted by $10\times$ due to its large scale. The 0.13B model takes roughly 178 hours on $16\times 32GB$ V100 GPUs.

4.3. Zero-shot Performance

For brevity, only the two largest FoundationGait versions (0.03B, 0.13B) are shown. These are compared against representative supervised [3, 10, 15] and self-supervised [12] methods across six widely used datasets in Tab 3.

First, compared with the SoTA self-supervised method GaitSSB [12], our 0.13B model achieves notable gains: +13.4% on the challenging in-the-wild Gait3D [100], +20.1% on the largest indoor OU-MVLP [71], and up to +16.8% on the clothing-diverse CCPG [39]. Notably, scaling up GaitSSB to 0.13B on WebGait-2M gains limited and even drops (e.g., -5.5% on OU-MVLP). **Hence, without method innovations like FoundationGait, simply enlarging model size is ineffective.**

Second, compared with popular supervised methods [3, 10, 15], our self-supervised FoundationGait remains highly competitive. On CASIA-B [93], it achieves comparable results under the normal (NM) condition. On the large-scale OU-MVLP [71] with over 5K testing subjects, it reaches 64.5% zero-shot rank-1 accuracy, nearly 70% of supervised performance. Remarkably, on the challenging Gait3D [100], our self-supervised 0.13B model even largely

Table 4. Fine-tuning Detail for Recognition. Batch size (p, q, j) denotes p subjects, q sequences each, and j frames per sequence.

| Dataset | Model | Batch Size | Milestones | Total | P |
|-----------------|-------|--------------|------------|-------|--------------|
| CCPG [39] | 0.03B | (16, 32, 30) | (2K) | 3K | [1, 2, 4, 8] |
| | 0.13B | (8, 32, 30) | (2K) | 3K | [1, 2, 4, 8] |
| Gait3D [100] | 0.03B | (128, 4, 30) | (3K) | 4K | [1, 2] |
| | 0.13B | (128, 4, 30) | (3K, 4K) | 5K | [1, 2] |
| CCGR-MINI [107] | 0.03B | (32, 16, 30) | (3K, 5K) | 6K | [1, 2, 4, 8] |
| | 0.13B | (32, 16, 30) | (3K, 5K) | 6K | [1, 2, 4, 8] |

Table 5. Gait Recognition. Fine-tuning on CCPG [39].

| Input | Method | Venue | CL | UP | DN | BG | Mean |
|-------|----------------------|----------|------|------|------|------|------|
| Ske. | GaitGraph2 [72] | CVPRW'22 | 5.0 | 5.3 | 5.8 | 6.2 | 5.6 |
| | Gait-TR [96] | ES'23 | 15.7 | 18.3 | 18.5 | 17.5 | 17.5 |
| | MSGG [60] | MTA'23 | 29.0 | 34.5 | 37.1 | 33.3 | 33.5 |
| | SkeletonGait [14] | AAAI'24 | 40.4 | 48.5 | 53.0 | 61.7 | 50.9 |
| Sil. | GaitSet [3] | AAAI'19 | 60.2 | 65.2 | 65.1 | 68.5 | 64.8 |
| | GaitPart [10] | CVPR'20 | 64.3 | 67.8 | 68.6 | 71.7 | 68.1 |
| | OGBase [39] | CVPR'23 | 52.1 | 57.3 | 60.1 | 63.3 | 58.2 |
| | GaitBase [13] | CVPR'23 | 71.6 | 75.0 | 76.8 | 78.6 | 75.5 |
| | DeepGaitV2 [15] | TPAMI'25 | 78.6 | 84.8 | 80.7 | 89.2 | 83.3 |
| | FoundationGait-0.03B | ours | 80.0 | 86.0 | 83.7 | 90.8 | 85.1 |
| | FoundationGait-0.13B | ours | 84.0 | 87.5 | 85.5 | 91.7 | 87.2 |

surpasses the famous supervised GaitSet [3] by +7.5%. These results highlight the great potential of gait pretraining, as well as the substantial progress achieved by FoundationGait.

4.4. Fine-tuning on Gait Recognition

Implementation. Following GaitSSB [12], we adopt layer-wise fine-tuning. Only the last two backbone blocks are fine-tuned ($\text{lr} = 0.001, 0.005$), while the projector and head use 0.01 and 0.1. SGD ($\text{lr} = 0.1$, momentum = 0.9) with a MultiStepLR scheduler is used. More details are in Tab. 4. **CCPG.** In Tab. 5, our 0.13B model delivers notable improvements in this challenging clothing-changing scene: +5.4% in full-changing (CL), +2.7% in ups-changing (UP),

Table 6. Gait Recognition. Fine-tuning on Gait3D [100].

| Method | Venue | Rank-1 | Rank-5 | mAP |
|----------------------|----------|-------------|-------------|-------------|
| GaitSet [3] | AAAI'19 | 36.7 | 58.3 | 30.0 |
| GaitPart [10] | CVPR'20 | 28.2 | 47.6 | 47.6 |
| GaitGL [42] | ICCV'21 | 29.7 | 48.5 | 22.3 |
| GaitContour [21] | WACV'25 | 25.3 | 41.3 | - |
| SMPLGait [100] | CVPR'22 | 46.3 | 64.5 | 37.2 |
| MTSGait [99] | MM'22 | 48.7 | 67.1 | 37.6 |
| QAGait [81] | AAAI'24 | 67.0 | 81.5 | 56.5 |
| GaitBase [13] | CVPR'23 | 64.6 | - | - |
| DANet [46] | CVPR'23 | 48.0 | 69.7 | - |
| GaitGCI [9] | CVPR'23 | 50.3 | 68.5 | 39.5 |
| DyGait [79] | ICCV'23 | 66.3 | 80.8 | 56.4 |
| HSTL [78] | ICCV'23 | 61.3 | 76.3 | 55.5 |
| VPNet [47] | CVPR'24 | 75.4 | 87.1 | - |
| DeepGaitV2 [15] | TPAMI'25 | 74.4 | 88.0 | 65.8 |
| CLTD [87] | ECCV'24 | 69.7 | 85.2 | - |
| GaitMoE [26] | ECCV'24 | 73.7 | - | 66.2 |
| Free Lunch [77] | ECCV'24 | 70.1 | - | 61.9 |
| VM-Gait [84] | WACV'25 | 75.4 | 87.5 | 66.4 |
| Mesh-Gait [83] | ArXiv'25 | 75.0 | 88.0 | 66.1 |
| FoundationGait-0.03B | ours | 77.7 | 89.6 | 71.1 |
| FoundationGait-0.13B | ours | 79.3 | 89.5 | 74.0 |

Table 7. Gait Recognition. Fine-tuning on CCGR-MINI [107].

| Method | Venue | Rank-1 | mAP | mINP |
|----------------------|----------|--------------|--------------|--------------|
| GaitSet [3] | AAAI'19 | 13.77 | 15.39 | 5.75 |
| GaitPart [10] | CVPR'20 | 8.02 | 10.12 | 3.52 |
| GaitGL [42] | ICCV'21 | 17.51 | 18.12 | 6.85 |
| GaitBase [13] | CVPR'23 | 26.99 | 24.89 | 9.72 |
| DeepGaitV2 [15] | TPAMI'25 | 39.37 | 36.01 | 16.77 |
| FoundationGait-0.03B | ours | 45.66 | 40.97 | 26.36 |
| FoundationGait-0.13B | ours | 53.25 | 48.00 | 33.29 |

+4.8% in pants-changing (DN), and +3.9% on average.

Gait3D. In Tab. 6, FoundationGait establishes a new SoTA on this challenging real world scene. Our 0.13B model achieves 79.3% Rank-1 and 74.0% mAP, significantly outperforming the previous best methods, VPNet [47] (+3.9% in Rank-1) and GaitMoE [26] (+7.8% in mAP).

CCGR-MINI. In this complex covariate setting, existing gait methods have long struggled (Rank-1 < 40%), but FoundationGait offers a significant breakthrough, *i.e.*, 45.66% / 53.25% on Rank-1 for our 0.03B / 0.13B model.

4.5. Fine-tuning on Healthcare Tasks

Implementation. Two settings (linear probing and fine-tuning) are evaluated. For linear probing, only the classification head is trained ($\text{lr} = 0.1$). For fine-tuning, the model is initialized from the linear probe stage and trained with layer-wise learning rates. The 0.03B model uses learning rates of 1×10^{-3} , 1×10^{-2} , and 1×10^{-1} for the backbone, projector, and head, respectively. Other settings follow Sec. 4.4. Batch size is (8, 8, 30), following the setting in Tab. 4. More details are in Tab. 8.

Linear Probe. As demonstrated in Tables 9, 10, and 11, the features extracted by FoundationGait exhibit strong linear separability across a variety of gait healthcare tasks. Specifically, for depression prediction [44] (+2.1% in F1

Table 8. Fine-tuning details for healthcare tasks.

| Mode | Dataset | Model | Milestones | Total | P |
|--------------|-------------------|-------|------------|-------|--------------|
| Linear Probe | Scoliosis1K [104] | 0.03B | (1K, 2K) | 3K | [1] |
| | | 0.13B | (1K, 2K) | 3K | [1] |
| | D-Gait [44] | 0.03B | (1K, 2K) | 3K | [1] |
| | | 0.13B | (3K, 4K) | 5K | [1] |
| | RA-GAR [75] | 0.03B | (1K) | 2K | [1] |
| Fine-tuning | Scoliosis1K [104] | 0.03B | (1K) | 2K | [1, 2, 4, 8] |
| | | 0.13B | (1K, 2K) | 3K | [1, 2, 4, 8] |
| | D-Gait [44] | 0.03B | (1K) | 2K | [1, 2, 4, 8] |
| | | 0.13B | (1K, 2K) | 3K | [1, 2, 4, 8] |
| | RA-GAR [75] | 0.03B | (1K) | 2K | [1, 2, 4, 8] |
| | | 0.13B | (1K) | 2K | [1, 2, 4, 8] |

Table 9. Scoliosis screening. Evaluation on Scoliosis1K [104].

| Mode | Method | Acc. | Precision | Recall | F1 |
|---------------|----------------------|-------------|-------------|-------------|-------------|
| Full-training | ScoNet [104] | 93.3 | 83.4 | 92.5 | 86.4 |
| | ScoNet-MT [104] | 95.2 | 80.2 | 96.6 | 84.9 |
| Linear Probe | FoundationGait-0.03B | 71.1 | 59.7 | 75.3 | 56.7 |
| | FoundationGait-0.13B | 73.5 | 61.0 | 68.5 | 56.9 |
| Fine-tuning | FoundationGait-0.03B | 97.3 | 95.4 | 88.9 | 91.7 |
| | FoundationGait-0.13B | 96.0 | 80.1 | 97.5 | 85.1 |

compared to GaitSet [3]) and gait attribute estimation [75] (+2.2% in F1 compared to CLIP-GAR [75]), Foundation-0.13B performs on par with, or even surpasses, previous SoTA methods that require full training. These results underscore the model’s superior ability to capture abundant and informative gait characteristics that are **already highly linearly separable in its feature space**, contributing to its strong generalizability across vision-based gait tasks.

Fine-tuning. After fine-tuning, FoundationGait demonstrates significant performance gains, with +6.8% in F1 on the Scoliosis1K [104] and +7.3% in F1 on the D-Gait [44] datasets. However, FoundationGait-0.13B tends to be overly optimistic in predicting positive cases, leading to high recall but lower accuracy compared to the 0.03B version on these class-imbalanced benchmarks. This suggests that the model size may influence the tendency to classify more samples as positive in long-tailed distributions. For the gait attribute estimation task (RA-GAR [75]), where labels are already well separable through linear probing of the pretrained FoundationGait, further fine-tuning yields no additional performance improvements.

In summary, FoundationGait demonstrates remarkable transferability and robustness across multiple gait healthcare tasks, achieving breakthrough performance with simple linear probing or fine-tuning in most cases. This highlights its potential as a unified foundation model for gait analysis, capable of delivering strong results even without task-specific designs on the fine-tuning strategy. Meanwhile, similar to recent approaches like LoRA [7] and Adapter [4], we believe that more refined fine-tuning strategies and task-specific optimizations could further expand the capabilities of FoundationGait, unlocking new avenues for advancements in healthcare gait analysis.

Table 10. Depression prediction. Evaluation on D-Gait [44].

| Mode | Method | Acc. | Precision | Recall | F1 |
|---------------|----------------------|-------------|-------------|-------------|-------------|
| Full-training | GaitBase [13] | - | 51.7 | 60.4 | 55.7 |
| | GaitSet [3] | - | 53.8 | 65.7 | 59.2 |
| | GaitGL [42] | - | 57.5 | 36.8 | 44.9 |
| Linear Probe | FoundationGait-0.03B | 66.3 | 57.7 | 57.8 | 57.8 |
| | FoundationGait-0.13B | 66.0 | 57.7 | 58.0 | 57.8 |
| Fine-tuning | FoundationGait-0.03B | 75.1 | 67.9 | 65.1 | 66.1 |
| | FoundationGait-0.13B | 72.2 | 66.0 | 67.4 | 66.5 |

Table 11. Gait Attribute Task. Evaluation on RA-GAR [75].

| Mode | Method | Instance-based | | | | Attr.-based |
|---------------|----------------------|----------------|-------------|-------------|-------------|-------------|
| | | Acc. | Prec. | Recall | F1 | mA |
| Full-training | GaitSet [3] | 84.4 | 75.7 | 66.1 | 70.2 | 64.3 |
| | GPGait [16] | 84.3 | 75.0 | 66.3 | 70.0 | 63.9 |
| | GAR-Net [67] | 84.3 | 77.4 | 74.7 | 73.2 | 62.2 |
| | DeepGaitV2 [15] | 85.0 | 76.6 | 66.7 | 70.9 | 61.7 |
| | CLIP-GAR [75] | 84.3 | 77.4 | 74.7 | 76.0 | 65.6 |
| Linear Probe | FoundationGait-0.03B | 85.2 | 78.6 | 76.4 | 77.4 | 64.3 |
| | FoundationGait-0.13B | 85.7 | 79.3 | 77.3 | 78.2 | 65.6 |
| Fine-tuning | FoundationGait-0.03B | 84.8 | 78.0 | 75.9 | 76.9 | 65.1 |
| | FoundationGait-0.13B | 84.7 | 78.1 | 75.5 | 76.7 | 65.7 |

Table 12. Exploring the effectiveness of part-aware training and its P , using FoundationGait-0.03B for pretraining.

| Method | P | CASIA-B [93] | | | OU-MVLP [71] | | Gait3D [100] | |
|------------|--------------|--------------|-------------|-------------|--------------|-------------|--------------|--|
| | | NM | BG | CL | Rank-1 | Rank-1 | mAP | |
| Crop | - | 69.5 | 58.1 | 26.4 | 25.7 | 16.4 | 11.1 | |
| Mask | - | 86.4 | 66.7 | 34.7 | 47.6 | 38.8 | 30.0 | |
| Part-aware | [1] | 84.9 | 66.3 | 30.7 | 44.3 | 42.1 | 32.3 | |
| | [1, 4] | 91.8 | 72.2 | 34.4 | 55.5 | 41.5 | 30.3 | |
| | [1, 2, 4, 8] | 92.0 | 72.9 | 39.4 | 57.0 | 41.1 | 30.0 | |

4.6. Ablation Study

We systematically evaluate: (a) the effectiveness of part-aware student and its hyperparameter P , (b) part-aware extensions in supervised models, (c) CNN vs. ViT as encoder, and (d) cross-modality generalization of FoundationGait. See **Supplementary Materials** for experiment details.

Part-aware Effectiveness. Compared to cropping [97] or masking silhouettes (Tab. 12), our part-aware student cleverly preserves all details, achieving stronger zero-shot results. Expanding P from [1] to [1, 2, 4, 8] causes a minor drop on the in-the-wild Gait3D [100] but clear gains on indoor CASIA-B [93] and OU-MVLP [71]. This likely reflects a stronger focus on local cues and is considered acceptable (+12.7% on OU-MVLP vs. -1.0% on Gait3D), so $P = [1, 2, 4, 8]$ is adopted.

Extension in Supervised Models. Beyond the self-supervised setting, can part-aware training be applied to large supervised models? Table 13 demonstrates that our part-aware training significantly benefits DeepGaitV2 with large model sizes. For example, the 0.13B version shows improvements of +5.5% on Gait3D and up to +20.2% on CASIA-B. This underscores the importance of preserving part diversity in large gait models, both in supervised and

Table 13. Extending part-aware training to DeepGaitV2 [15], where w/ denotes the use of part-aware training.

| Model | w/ | CASIA-B [93] | | | Gait3D [100] | |
|------------|----|--------------|-------------|-------------|--------------|-------------|
| | | NM | BG | CL | Rank-1 | mAP |
| DeepGaitV2 | × | 84.5 | 72.3 | 46.5 | 73.3 | 65.6 |
| | ✓ | 92.4 | 87.0 | 66.2 | 74.3 | 67.3 |
| DeepGaitV2 | × | 79.2 | 68.0 | 42.2 | 70.8 | 64.0 |
| | ✓ | 90.0 | 81.4 | 62.4 | 76.3 | 68.7 |

Table 14. Replacing the last two CNN blocks with ViT.

| Block | Depths | CASIA-B [93] | | | Gait3D [100] | |
|---------|--------|--------------|-------------|-------------|--------------|-------------|
| | | NM | BG | CL | Rank-1 | mAP |
| ViT [8] | (12) | 87.1 | 68.2 | 26.3 | 28.3 | 19.3 |
| CNN | (8, 4) | 92.0 | 72.9 | 39.4 | 41.1 | 30.0 |

Table 15. Fine-tuning FoundationGait (FG) on Gait3D [100] with taking the unseen human parsing as input.

| Modality | Method | Venue | Rank-1 | Rank-5 | mAP |
|----------|------------------|----------|-------------|-------------|-------------|
| Sil. | VPNet [47] | CVPR'24 | 75.4 | 87.1 | - |
| | DeepGaitV2 [13] | TPAMI'25 | 74.4 | 88.0 | 65.8 |
| | GaitMoE [26] | ECCV'24 | 73.7 | - | 66.2 |
| Parsing | FG-0.03B | ours | 82.0 | 91.6 | 76.1 |
| | FG-0.13B | ours | 83.8 | 92.7 | 79.3 |
| Sil. | XGait [102] | MM'24 | 80.5 | 91.9 | 73.3 |
| | MultiGait++ [31] | AAAI'25 | 85.4 | 94.9 | 80.5 |
| +Parsing | FG-0.03B | ours | 84.2 | 92.8 | 78.8 |
| | FG-0.13B | ours | 86.5 | 93.8 | 82.6 |

self-supervised settings, and our part-aware training offers a flexible and promising solution.

ViT Replacement. Following SwinGait [15], we replace the last two CNN blocks (of sizes (8, 4)) in FoundationGait-0.03B with a 12-layer ViT block, resulting in a noticeable performance drop (see Table 14). The reasons for this decline remain unclear and are not specific to FoundationGait. In fact, CNN-based architectures continue to dominate vision-based gait methods [15].

Cross-modality Generalization. Although FoundationGait has never been pretrained on the gait modality of human parsing, we found that it performs well in both parsing-only and multi-modal settings after fine-tuning (Tab. 15). This highlights FoundationGait’s ability to transform raw pixel-based shapes, across diverse data types, into fine-grained semantic features.

5. Conclusion and Limitations

We introduce FoundationGait, a scalable self-supervised gait foundation model that addresses key challenges in size scalability and cross-task generalization. FoundationGait demonstrates that a unified model can effectively tackle both recognition and healthcare tasks, paving the way for more versatile, practical applications of gait biometrics.

In the end, two issues warrant further investigation:

ViT-based Gait Foundation Model. This issue is crucial for bridging gait-specific foundation models with those

from other domains, particularly LLMs [74], yet it remains largely unexplored within the gait community.

FoundationGait-1B. Due to computational constraints, we only scaled the model up by $21\times$ to 0.13B and verified that its performance still follows the scaling-law trend in Fig. 2. Can we scale it beyond 1B? This is an ongoing goal.

References

- [1] Landing AI. Domain-specific large vision models (lvms), 2024. Accessed: 2025-11-07. [1](#)
- [2] Emily M Bender, Timnit Gebru, Angelina McMillan-Major, and Shmargaret Shmitchell. On the dangers of stochastic parrots: Can language models be too big? In *Proceedings of the 2021 ACM conference on fairness, accountability, and transparency*, pages 610–623, 2021. [4](#)
- [3] Hanqing Chao, Yiwei He, Junping Zhang, and Jianfeng Feng. Gaitset: Regarding gait as a set for cross-view gait recognition. In *Proceedings of the AAAI Conference on Artificial Intelligence (AAAI)*, pages 8126–8133, 2019. [3](#), [6](#), [7](#), [8](#)
- [4] Hao Chen, Ran Tao, Han Zhang, Yidong Wang, Xiang Li, Wei Ye, Jindong Wang, Guosheng Hu, and Marios Savvides. Conv-adapter: Exploring parameter efficient transfer learning for convnets. In *Proceedings of the IEEE/CVF Conference on Computer Vision and Pattern Recognition (CVPR)*, pages 1551–1561, 2024. [7](#)
- [5] Xinlei Chen and Kaiming He. Exploring simple siamese representation learning. In *Proceedings of the IEEE/CVF Conference on Computer Vision and Pattern Recognition (CVPR)*, pages 15750–15758, 2021. [2](#), [3](#)
- [6] Jiankang Deng, Jia Guo, Niannan Xue, and Stefanos Zafeiriou. Arcface: Additive angular margin loss for deep face recognition. In *Proceedings of the IEEE/CVF Conference on Computer Vision and Pattern Recognition (CVPR)*, pages 4690–4699, 2019. [3](#)
- [7] Chuntao Ding, Xu Cao, Jianhang Xie, Linlin Fan, Shangguang Wang, and Zhichao Lu. Lora-c: Parameter-efficient fine-tuning of robust cnn for iot devices. *arXiv preprint arXiv:2410.16954*, 2024. [7](#)
- [8] Alexey Dosovitskiy. An image is worth 16x16 words: Transformers for image recognition at scale. *arXiv preprint arXiv:2010.11929*, 2020. [8](#)
- [9] Huanzhang Dou, Pengyi Zhang, Wei Su, Yunlong Yu, Yining Lin, and Xi Li. Gaitgci: Generative counterfactual intervention for gait recognition. In *Proceedings of the IEEE/CVF Conference on Computer Vision and Pattern Recognition (CVPR)*, pages 5578–5588, 2023. [2](#), [7](#)
- [10] Chao Fan, Yunjie Peng, Chunshui Cao, Xu Liu, Saihui Hou, Jiannan Chi, Yongzhen Huang, Qing Li, and Zhiqiang He. Gaitpart: Temporal part-based model for gait recognition. In *Proceedings of the IEEE/CVF Conference on Computer Vision and Pattern Recognition (CVPR)*, pages 14225–14233, 2020. [2](#), [4](#), [6](#), [7](#)
- [11] Chao Fan, Saihui Hou, Yongzhen Huang, and Shiqi Yu. Exploring deep models for practical gait recognition. *arXiv preprint arXiv:2303.03301*, 2023. [4](#)
- [12] Chao Fan, Saihui Hou, Jilong Wang, Yongzhen Huang, and Shiqi Yu. Learning gait representation from massive unlabelled walking videos: A benchmark. *IEEE Transactions on Pattern Analysis and Machine Intelligence (TPAMI)*, 45 (12):14920–14937, 2023. [1](#), [2](#), [3](#), [4](#), [5](#), [6](#)
- [13] Chao Fan, Junhao Liang, Chuanfu Shen, Saihui Hou, Yongzhen Huang, and Shiqi Yu. Opengait: Revisiting gait recognition towards better practicality. In *Proceedings of the IEEE/CVF Conference on Computer Vision and Pattern Recognition (CVPR)*, pages 9707–9716, 2023. [3](#), [5](#), [6](#), [7](#), [8](#)
- [14] Chao Fan, Jingzhe Ma, Dongyang Jin, Chuanfu Shen, and Shiqi Yu. Skeletongait: Gait recognition using skeleton maps. In *Proceedings of the AAAI Conference on Artificial Intelligence (AAAI)*, pages 1662–1669, 2024. [2](#), [6](#)
- [15] Chao Fan, Saihui Hou, Junhao Liang, Chuanfu Shen, Jingzhe Ma, Dongyang Jin, Yongzhen Huang, and Shiqi Yu. Opengait: A comprehensive benchmark study for gait recognition towards better practicality. *IEEE Transactions on Pattern Analysis and Machine Intelligence (TPAMI)*, 2025. [2](#), [3](#), [4](#), [5](#), [6](#), [7](#), [8](#)
- [16] Yang Fu, Shibe Meng, Saihui Hou, Xuecai Hu, and Yongzhen Huang. Gpgait: Generalized pose-based gait recognition. In *Proceedings of the IEEE/CVF International Conference on Computer Vision (ICCV)*, pages 19595–19604, 2023. [8](#)
- [17] Jean-Bastien Grill, Florian Strub, Florent Altché, Corentin Tallec, Pierre Richemond, Elena Buchatskaya, Carl Dohersch, Bernardo Avila Pires, Zhaohan Guo, Mohammad Gheshlaghi Azar, et al. Bootstrap your own latent—a new approach to self-supervised learning. *Advances in Neural Information Processing Systems (NeurIPS)*, 33:21271–21284, 2020. [4](#)
- [18] Zhaopeng Gu, Bingke Zhu, Guibo Zhu, Yingying Chen, Ming Tang, and Jinqiao Wang. Anomalygpt: detecting industrial anomalies using large vision-language models. In *Proceedings of the AAAI Conference on Artificial Intelligence (AAAI)*, 2024. [1](#), [3](#)
- [19] Hongji Guo and Qiang Ji. Physics-augmented autoencoder for 3d skeleton-based gait recognition. In *Proceedings of the IEEE/CVF International Conference on Computer Vision (ICCV)*, pages 19627–19638, 2023. [2](#)
- [20] Xin Guo, Jiangwei Lao, Bo Dang, Yingying Zhang, Lei Yu, Lixiang Ru, Liheng Zhong, Ziyuan Huang, Kang Wu, Dingxiang Hu, et al. Skysense: A multi-modal remote sensing foundation model towards universal interpretation for earth observation imagery. In *Proceedings of the IEEE/CVF Conference on Computer Vision and Pattern Recognition (CVPR)*, pages 27672–27683, 2024. [1](#), [3](#)
- [21] Yuxiang Guo, Anshul Shah, Jiang Liu, Ayush Gupta, Rama Chellappa, and Cheng Peng. Gaitcontour: Efficient gait recognition based on a contour-pose representation. In *IEEE Winter Conference on Applications of Computer Vision*, pages 1051–1061. IEEE, 2025. [2](#), [7](#)
- [22] Ayush Gupta and Rama Chellappa. You can run but not hide: Improving gait recognition with intrinsic occlusion type awareness. In *IEEE Winter Conference on Applications of Computer Vision*, pages 5893–5902, 2024. [2](#)

- [23] Ayush Gupta and Rama Chellappa. Mimicgait: A model agnostic approach for occluded gait recognition using correlational knowledge distillation. In *IEEE Winter Conference on Applications of Computer Vision*, pages 4757–4766. IEEE, 2025.
- [24] Ayush Gupta, Siyuan Huang, and Rama Chellappa. Mind the gap: Bridging occlusion in gait recognition via residual gap correction. In *IEEE International Joint Conference on Biometrics (IJCB)*, 2025. 2
- [25] Michael Gutmann and Aapo Hyvärinen. Noise-contrastive estimation: A new estimation principle for unnormalized statistical models. In *Proceedings of the thirteenth international conference on artificial intelligence and statistics*, pages 297–304, 2010. 5
- [26] Panjian Huang, Yunjie Peng, Saihui Hou, Chunshui Cao, Xu Liu, Zhiqiang He, and Yongzhen Huang. Occluded gait recognition with mixture of experts: an action detection perspective. In *Proceedings of the European Conference on Computer Vision (ECCV)*, pages 380–397. Springer, 2024. 2, 7, 8
- [27] Panjian Huang, Saihui Hou, Chunshui Cao, Xu Liu, and Yongzhen Huang. Vocabulary-guided gait recognition. In *Advances in Neural Information Processing Systems (NeurIPS)*, 2025. 2
- [28] Panjian Huang, Saihui Hou, Junzhou Huang, and Yongzhen Huang. Learning a unified template for gait recognition. In *Proceedings of the IEEE/CVF International Conference on Computer Vision (ICCV)*, pages 12459–12469, 2025. 2
- [29] Zhizhong Huang and Xiaoming Liu. Generalizable object re-identification via visual in-context prompting. In *Proceedings of the IEEE/CVF International Conference on Computer Vision (ICCV)*, pages 22539–22550, 2025. 2
- [30] Zhanbo Huang, Xiaoming Liu, and Yu Kong. H-more: Learning human-centric motion representation for action analysis. In *Proceedings of the IEEE/CVF Conference on Computer Vision and Pattern Recognition (CVPR)*, pages 22702–22713, 2025. 2
- [31] Dongyang Jin, Chao Fan, Weihua Chen, and Shiqi Yu. Exploring more from multiple gait modalities for human identification. In *Proceedings of the AAAI Conference on Artificial Intelligence (AAAI)*, pages 4120–4128, 2025. 2, 8
- [32] Dongyang Jin, Chao Fan, Jingzhe Ma, Jingkai Zhou, Weihua Chen, and Shiqi Yu. On denoising walking videos for gait recognition. In *Proceedings of the IEEE/CVF Conference on Computer Vision and Pattern Recognition (CVPR)*, pages 12347–12357, 2025. 1, 2
- [33] Jared Kaplan, Sam McCandlish, Tom Henighan, Tom B Brown, Benjamin Chess, Rewon Child, Scott Gray, Alec Radford, Jeffrey Wu, and Dario Amodei. Scaling laws for neural language models. *arXiv preprint arXiv:2001.08361*, 2020. 2, 3
- [34] Rawal Khirodkar, Timur Bagautdinov, Julieta Martinez, Su Zhaoen, Austin James, Peter Selednik, Stuart Anderson, and Shunsuke Saito. Sapiens: Foundation for human vision models. In *European Conference on Computer Vision*, pages 206–228. Springer, 2024. 1, 3
- [35] Minchul Kim, Anil Jain, and Xiaoming Liu. 50 years of automated face recognition. *arXiv preprint arXiv:2505.24247*, 2025. 3
- [36] Minchul Kim, Dingqiang Ye, Yiyang Su, Feng Liu, and Xiaoming Liu. Sapiensid: Foundation for human recognition. In *Proceedings of the IEEE/CVF Conference on Computer Vision and Pattern Recognition (CVPR)*, pages 13937–13947, 2025. 1, 3
- [37] Alexander Kirillov, Eric Mintun, Nikhila Ravi, Hanzi Mao, Chloe Rolland, Laura Gustafson, Tete Xiao, Spencer Whitehead, Alexander C Berg, Wan-Yen Lo, et al. Segment anything. In *Proceedings of the IEEE/CVF International Conference on Computer Vision (ICCV)*, pages 4015–4026, 2023. 1, 3
- [38] Markus Rafael Konieczny, Hüsseyin Senyurt, and Rüdiger Krauspe. Epidemiology of adolescent idiopathic scoliosis. *Journal of Children’s Orthopaedics*, 7(1):3–9, 2013. PMID: 24432052. 2
- [39] Weijia Li, Saihui Hou, Chunjie Zhang, Chunshui Cao, Xu Liu, Yongzhen Huang, and Yao Zhao. An in-depth exploration of person re-identification and gait recognition in cloth-changing conditions. In *Proceedings of the IEEE/CVF Conference on Computer Vision and Pattern Recognition (CVPR)*, pages 13824–13833, 2023. 2, 4, 5, 6
- [40] Junhao Liang, Chao Fan, Saihui Hou, Chuanfu Shen, Yongzhen Huang, and Shiqi Yu. Gaitedge: Beyond plain end-to-end gait recognition for better practicality. In *Proceedings of the European Conference on Computer Vision (ECCV)*, pages 375–390. Springer, 2022. 2
- [41] Beibei Lin, Shunli Zhang, and Xin Yu. Gait recognition via effective global-local feature representation and local temporal aggregation. In *Proceedings of the IEEE/CVF International Conference on Computer Vision (ICCV)*, pages 14648–14656, 2021. 2
- [42] Beibei Lin, Shunli Zhang, Ming Wang, Lincheng Li, and Xin Yu. Gaitgl: Learning discriminative global-local feature representations for gait recognition. *arXiv preprint arXiv:2208.01380*, 2022. 7, 8
- [43] Feng Liu, Nicholas Chimitt, Lanqing Guo, Jitesh Jain, Aditya Kane, Minchul Kim, Wes Robbins, Yiyang Su, Dingqiang Ye, Xingguang Zhang, et al. Person recognition at altitude and range: Fusion of face, body shape and gait. *arXiv preprint arXiv:2505.04616*, 2025. 2
- [44] Xiaotong Liu, Qiong Li, Saihui Hou, Min Ren, Xuecai Hu, and Yongzhen Huang. Depression risk recognition based on gait: A benchmark. *Neurocomputing*, 596:128045, 2024. 1, 2, 5, 7, 8
- [45] Ze Liu, Yutong Lin, Yue Cao, Han Hu, Yixuan Wei, Zheng Zhang, Stephen Lin, and Baining Guo. Swin transformer: Hierarchical vision transformer using shifted windows. In *Proceedings of the IEEE/CVF International Conference on Computer Vision (ICCV)*, pages 10012–10022, 2021. 5
- [46] Kang Ma, Ying Fu, Dezhi Zheng, Chunshui Cao, Xuecai Hu, and Yongzhen Huang. Dynamic aggregated network for gait recognition. In *Proceedings of the IEEE/CVF Conference on Computer Vision and Pattern Recognition (CVPR)*, pages 22076–22085, 2023. 2, 7

- [47] Kang Ma, Ying Fu, Chunshui Cao, Saihui Hou, Yongzhen Huang, and Dezhi Zheng. Learning visual prompt for gait recognition. In *Proceedings of the IEEE/CVF Conference on Computer Vision and Pattern Recognition (CVPR)*, pages 593–603, 2024. 7, 8
- [48] Kangfu Mei, Mo Zhou, and Vishal M Patel. Field-dit: Diffusion transformer on unified video, 3d, and game field generation. In *Proceedings of the International Conference on Learning Representations (ICLR)*, 2025. 2
- [49] Yiqun Mei, Mingming He, Li Ma, Julien Philip, Wenqi Xian, David M George, Xueming Yu, Gabriel Dedic, Ahmet Levent Taşel, Ning Yu, et al. Lux post facto: Learning portrait performance relighting with conditional video diffusion and a hybrid dataset. In *Proceedings of the IEEE/CVF Conference on Computer Vision and Pattern Recognition (CVPR)*, pages 5510–5522, 2025. 3
- [50] Shibe Meng, Saihui Hou, Yang Fu, Xuecai Hu, Junzhou Huang, and Yongzhen Huang. Seeing from magic mirror: Contrastive learning from reconstruction for pose-based gait recognition. In *Proceedings of the 33rd ACM International Conference on Multimedia*, pages 7719–7728, 2025. 2
- [51] Nithin Gopalakrishnan Nair, Kartik Narayan, Maitreya Suin, Ram Prabhakar Kathirvel, Jennifer Xu, Soraya Stevens, Joshua Gleason, Nathan Shnidman, Rama Chellappa, and Vishal Patel. Improved representation learning for unconstrained face recognition. In *International Conference on Automatic Face and Gesture Recognition (FG)*, pages 1–10. IEEE, 2025. 3
- [52] Kartik Narayan, Nithin Gopalakrishnan Nair, Jennifer Xu, Rama Chellappa, and Vishal M Patel. Petalface: Parameter efficient transfer learning for low-resolution face recognition. In *IEEE Winter Conference on Applications of Computer Vision*, pages 804–814. IEEE, 2025.
- [53] Kartik Narayan, Vibashan VS, Rama Chellappa, and Vishal M Patel. Facexformer: A unified transformer for facial analysis. In *Proceedings of the IEEE/CVF International Conference on Computer Vision (ICCV)*, pages 11369–11382, 2025. 3
- [54] Mark S Nixon, Tieniu Tan, and Rama Chellappa. *Human identification based on gait*. Springer Science & Business Media, 2010. 1
- [55] Niyogi and Adelson. Analyzing and recognizing walking figures in xyt. In *Proceedings of the IEEE/CVF Conference on Computer Vision and Pattern Recognition (CVPR)*, pages 469–474. IEEE, 1994. 1, 2
- [56] National Institute of Mental Health. Major depression. <https://www.nimh.nih.gov/health/statistics/major-depression>, 2022. Accessed: 2023-11-08. 2
- [57] Maxime Oquab, Timothée Darcet, Théo Moutakanni, Huy Vo, Marc Szafraniec, Vasil Khalidov, Pierre Fernandez, Daniel Haziza, Francisco Massa, Alaaeldin El-Nouby, et al. Dinov2: Learning robust visual features without supervision. *arXiv preprint arXiv:2304.07193*, 2023. 1, 3
- [58] William Peebles and Saining Xie. Scalable diffusion models with transformers. In *Proceedings of the IEEE/CVF International Conference on Computer Vision (ICCV)*, pages 4172–4182, 2023. 1
- [59] Guozhen Peng, Yunhong Wang, Yuwei Zhao, Shaoxiong Zhang, and Annan Li. Glgait: a global-local temporal receptive field network for gait recognition in the wild. In *Proceedings of the ACM International Conference on Multimedia (ACM MM)*, pages 826–835, 2024. 2
- [60] Yunjie Peng, Kang Ma, Yang Zhang, and Zhiqiang He. Learning rich features for gait recognition by integrating skeletons and silhouettes. *Multimedia Tools and Applications*, 83(3):7273–7294, 2024. 6
- [61] Alec Radford, Jong Wook Kim, Chris Hallacy, Aditya Ramesh, Gabriel Goh, Sandhini Agarwal, Girish Sastry, Amanda Askell, Pamela Mishkin, Jack Clark, et al. Learning transferable visual models from natural language supervision. In *International conference on machine learning (ICML)*, pages 8748–8763. PmLR, 2021. 2, 3
- [62] Rajeev Ranjan, Vishal M Patel, and Rama Chellappa. Hyperface: A deep multi-task learning framework for face detection, landmark localization, pose estimation, and gender recognition. *IEEE Transactions on Pattern Analysis and Machine Intelligence (TPAMI)*, 41(1):121–135, 2017. 3
- [63] Robin Rombach, Andreas Blattmann, Dominik Lorenz, Patrick Esser, and Björn Ommer. High-resolution image synthesis with latent diffusion models. In *Proceedings of the IEEE/CVF Conference on Computer Vision and Pattern Recognition (CVPR)*, pages 10684–10695, 2022. 1
- [64] Chuanfu Shen, Chao Fan, Wei Wu, Rui Wang, George Q Huang, and Shiqi Yu. Lidargait: Benchmarking 3d gait recognition with point clouds. In *Proceedings of the IEEE/CVF Conference on Computer Vision and Pattern Recognition (CVPR)*, pages 1054–1063, 2023. 2, 5, 6
- [65] Chuanfu Shen, Rui Wang, Lixin Duan, and Shiqi Yu. Lidargait++: Learning local features and size awareness from lidar point clouds for 3d gait recognition. In *Proceedings of the IEEE/CVF Conference on Computer Vision and Pattern Recognition (CVPR)*, pages 6627–6636, 2025. 2
- [66] Chunfeng Song, Yongzhen Huang, Weining Wang, and Liang Wang. Casia-e: A large comprehensive dataset for gait recognition. *IEEE Transactions on Pattern Analysis and Machine Intelligence (TPAMI)*, 45(3):2801–2815, 2022. 2, 5
- [67] Xu Song, Saihui Hou, Yan Huang, Chunshui Cao, Xu Liu, Yongzhen Huang, and Caifeng Shan. Gait attribute recognition: A new benchmark for learning richer attributes from human gait patterns. *IEEE Transactions on Information Forensics and Security*, 19:1–14, 2023. 8
- [68] Samuel Stevens, Jiaman Wu, Matthew J Thompson, Elizabeth G Campolongo, Chan Hee Song, David Edward Carlyn, Li Dong, Wasila M Dahdul, Charles Stewart, Tanya Berger-Wolf, et al. Bioclip: A vision foundation model for the tree of life. In *Proceedings of the IEEE/CVF Conference on Computer Vision and Pattern Recognition (CVPR)*, pages 19412–19424, 2024. 1
- [69] Yiyang Su, Minchul Kim, Feng Liu, Anil Jain, and Xiaoming Liu. Open-set biometrics: Beyond good closed-set models. In *Proceedings of the European Conference on*

- Computer Vision (ECCV)*, pages 243–261. Springer, 2024. 2
- [70] Yiyang Su, Yunping Shi, Feng Liu, and Xiaoming Liu. Hamobe: Hierarchical and adaptive mixture of biometric experts for video-based person reid. In *Proceedings of the IEEE/CVF International Conference on Computer Vision (ICCV)*, pages 11525–11536, 2025. 3
- [71] Noriko Takemura, Yasushi Makihara, Daigo Muramatsu, Tomio Echigo, and Yasushi Yagi. Multi-view large population gait dataset and its performance evaluation for cross-view gait recognition. *IPSI transactions on Computer Vision and Applications*, 10(1):4, 2018. 2, 5, 6, 8
- [72] Torben Teepe, Ali Khan, Johannes Gilg, Fabian Herzog, Stefan Hörmann, and Gerhard Rigoll. Gaitgraph: Graph convolutional network for skeleton-based gait recognition. In *Proceedings of the IEEE International Conference on Image Processing (ICIP)*, pages 2314–2318. IEEE, 2021. 6
- [73] Pavan Turaga, Rama Chellappa, Venkatramana S Subrahmanian, and Octavian Udrea. Machine recognition of human activities: A survey. *IEEE Transactions on Circuits and Systems for Video Technology (TCSVT)*, 18(11):1473–1488, 2008. 1
- [74] Ashish Vaswani, Noam Shazeer, Niki Parmar, Jakob Uszkoreit, Llion Jones, Aidan N Gomez, Łukasz Kaiser, and Illia Polosukhin. Attention is all you need. *Advances in Neural Information Processing Systems (NeurIPS)*, 30, 2017. 9
- [75] Chenye Wang, Saihui Hou, Aoqi Li, Qingyuan Cai, and Yongzhen Huang. Ra-gar: A richly annotated benchmark for gait attribute recognition. In *Proceedings of the AAAI Conference on Artificial Intelligence (AAAI)*, pages 7591–7599, 2025. 1, 2, 3, 5, 7, 8
- [76] Jilong Wang, Saihui Hou, Yan Huang, Chunshui Cao, Xu Liu, Yongzhen Huang, and Liang Wang. Causal intervention for sparse-view gait recognition. In *Proceedings of the ACM International Conference on Multimedia (ACM MM)*, pages 77–85, 2023. 2
- [77] Jilong Wang, Saihui Hou, Yan Huang, Chunshui Cao, Xu Liu, Yongzhen Huang, Tianzhu Zhang, and Liang Wang. Free lunch for gait recognition: A novel relation descriptor. In *Proceedings of the European Conference on Computer Vision (ECCV)*, pages 39–56. Springer, 2024. 7
- [78] Lei Wang, Bo Liu, Fangfang Liang, and Bincheng Wang. Hierarchical spatio-temporal representation learning for gait recognition. In *Proceedings of the IEEE/CVF International Conference on Computer Vision (ICCV)*, pages 19582–19592. IEEE, 2023. 2, 7
- [79] Ming Wang, Xianda Guo, Beibei Lin, Tian Yang, Zheng Zhu, Lincheng Li, Shunli Zhang, and Xin Yu. Dygait: Exploiting dynamic representations for high-performance gait recognition. In *Proceedings of the IEEE/CVF International Conference on Computer Vision (ICCV)*, pages 13424–13433, 2023. 2, 7
- [80] Zengbin Wang, Saihui Hou, Man Zhang, Xu Liu, Chunshui Cao, and Yongzhen Huang. Gaitparsing: Human semantic parsing for gait recognition. *IEEE Transactions on Multimedia (TMM)*, 26:4736–4748, 2023. 2
- [81] Zengbin Wang, Saihui Hou, Man Zhang, Xu Liu, Chunshui Cao, Yongzhen Huang, Peipei Li, and Shibiao Xu. Qagait: Revisit gait recognition from a quality perspective. In *Proceedings of the AAAI Conference on Artificial Intelligence (AAAI)*, pages 5785–5793, 2024. 2, 7
- [82] Zhao-Yang Wang, Jiang Liu, Ram Prabhakar Kathirvel, Chun Pong Lau, and Rama Chellappa. Hypergait: A video-based multitask network for gait recognition and human attribute estimation at range and altitude. In *IEEE International Joint Conference on Biometrics (IJCB)*, pages 1–9. IEEE, 2024. 3
- [83] Zhao-Yang Wang, Jieneng Chen, Jiang Liu, Yuxiang Guo, and Rama Chellappa. Mesh-gait: A unified framework for gait recognition through multi-modal representation learning from 2d silhouettes. *arXiv preprint arXiv:2510.10406*, 2025. 2, 7
- [84] Zhao-Yang Wang, Jiang Liu, Jieneng Chen, and Rama Chellappa. Vm-gait: Multi-modal 3d representation based on virtual marker for gait recognition. In *IEEE Winter Conference on Applications of Computer Vision*, pages 5326–5335. IEEE, 2025. 2, 7
- [85] Zhao-Yang Wang, Jiang Liu, Yuxiang Guo, Jieneng Chen, and Rama Chellappa. Unigait: A unified transformer-based multitask framework for gait analysis in the wild. In *International Conference on Automatic Face and Gesture Recognition (FG)*, pages 1–9. IEEE, 2025. 3
- [86] Zhao-Yang Wang, Zhimin Shao, Jieneng Chen, and Rama Chellappa. Combo-gait: Unified transformer framework for multi-modal gait recognition and attribute analysis. *arXiv preprint arXiv:2510.10417*, 2025. 2
- [87] Haijun Xiong, Bin Feng, Xinggang Wang, and Wenyu Liu. Causality-inspired discriminative feature learning in triple domains for gait recognition. In *Proceedings of the European Conference on Computer Vision (ECCV)*, pages 251–270. Springer, 2024. 2, 7
- [88] Chi Xu, Yasushi Makihara, Xiang Li, and Yasushi Yagi. Occlusion-aware human mesh model-based gait recognition. *IEEE transactions on information forensics and security*, 18:1309–1321, 2023. 2
- [89] Jiacong Xu, Shao-Yuan Lo, Bardia Safaei, Vishal M Patel, and Isht Dwivedi. Towards zero-shot anomaly detection and reasoning with multimodal large language models. In *Proceedings of the IEEE/CVF Conference on Computer Vision and Pattern Recognition (CVPR)*, pages 20370–20382, 2025. 3
- [90] Dingqiang Ye, Jingzhe Ma, Chao Fan, and Shiqi Yu. Gaite-diter: Attribute editing for gait representation learning. *arXiv e-prints*, pages arXiv–2303, 2023. 2
- [91] Dingqiang Ye, Chao Fan, Jingzhe Ma, Xiaoming Liu, and Shiqi Yu. Biggait: Learning gait representation you want by large vision models. In *Proceedings of the IEEE/CVF Conference on Computer Vision and Pattern Recognition (CVPR)*, pages 200–210, 2024. 1, 2
- [92] Dingqiang Ye, Chao Fan, Zhanbo Huang, Chengwen Luo, Jianqiang Li, Shiqi Yu, and Xiaoming Liu. Biggergait: Unlocking gait recognition with layer-wise representations from large vision models. *Advances in Neural Information Processing Systems (NeurIPS)*, 2025. 1, 2

- [93] Shiqi Yu, Daoliang Tan, and Tieniu Tan. A framework for evaluating the effect of view angle, clothing and carrying condition on gait recognition. In *Proceedings of the International Conference on Pattern Recognition (ICPR)*, pages 441–444. IEEE, 2006. [2](#), [5](#), [6](#), [8](#)
- [94] Weichen Yu, Hongyuan Yu, Yan Huang, and Liang Wang. Generalized inter-class loss for gait recognition. In *Proceedings of the ACM International Conference on Multimedia (ACM MM)*, pages 141–150, 2022. [2](#)
- [95] Chiyuan Zhang, Samy Bengio, Moritz Hardt, Benjamin Recht, and Oriol Vinyals. Understanding deep learning requires rethinking generalization. *arXiv preprint arXiv:1611.03530*, 2016. [4](#)
- [96] Cun Zhang, Xing-Peng Chen, Guo-Qiang Han, and Xiang-Jie Liu. Spatial transformer network on skeleton-based gait recognition. *Expert Systems*, 40(6):e13244, 2023. [6](#)
- [97] Ke Zhang, Tianyu Ding, Jiachen Jiang, Tianyi Chen, Ilya Zharkov, Vishal M Patel, and Luming Liang. Procrop: Learning aesthetic image cropping from professional compositions. *Proceedings of the AAAI Conference on Artificial Intelligence (AAAI)*, 2026. [8](#)
- [98] Shaoxiong Zhang, Yunhong Wang, and Annan Li. Cross-view gait recognition with deep universal linear embeddings. In *Proceedings of the IEEE/CVF Conference on Computer Vision and Pattern Recognition (CVPR)*, pages 9095–9104, 2021. [2](#)
- [99] Jinkai Zheng, Xinchun Liu, Xiaoyan Gu, Yaoqi Sun, Chuang Gan, Jiyong Zhang, Wu Liu, and Chenggang Yan. Gait recognition in the wild with multi-hop temporal switch. In *Proceedings of the 30th ACM International Conference on Multimedia*, pages 6136–6145, 2022. [7](#)
- [100] Jinkai Zheng, Xinchun Liu, Wu Liu, Lingxiao He, Chenggang Yan, and Tao Mei. Gait recognition in the wild with dense 3d representations and a benchmark. In *Proceedings of the IEEE/CVF Conference on Computer Vision and Pattern Recognition (CVPR)*, pages 20228–20237, 2022. [2](#), [4](#), [5](#), [6](#), [7](#), [8](#)
- [101] Jinkai Zheng, Xinchun Liu, Shuai Wang, Lihao Wang, Chenggang Yan, and Wu Liu. Parsing is all you need for accurate gait recognition in the wild. In *Proceedings of the ACM International Conference on Multimedia (ACM MM)*, pages 116–124, 2023. [2](#)
- [102] Jinkai Zheng, Xinchun Liu, Boyue Zhang, Chenggang Yan, Jiyong Zhang, Wu Liu, and Yongdong Zhang. It takes two: Accurate gait recognition in the wild via cross-granularity alignment. In *Proceedings of the ACM International Conference on Multimedia (ACM MM)*, pages 8786–8794, 2024. [8](#)
- [103] Mo Zhou, Keren Ye, Viraj Shah, Kangfu Mei, Mauricio Delbracio, Peyman Milanfar, Vishal M Patel, and Hossein Talebi. Reference-guided identity preserving face restoration. *arXiv preprint arXiv:2505.21905*, 2025. [3](#)
- [104] Zirui Zhou, Junhao Liang, Zizhao Peng, Chao Fan, Fengwei An, and Shiqi Yu. Gait patterns as biomarkers: A video-based approach for classifying scoliosis. In *International conference on medical image computing and computer-assisted intervention (MICCAI)*, pages 284–294. Springer, 2024. [1](#), [2](#), [3](#), [5](#), [7](#)
- [105] Jie Zhu, Yiyang Su, Minchul Kim, Anil Jain, and Xiaoming Liu. A quality-guided mixture of score-fusion experts framework for human recognition. In *Proceedings of the IEEE/CVF International Conference on Computer Vision (ICCV)*, pages 13076–13086, 2025. [3](#)
- [106] Zheng Zhu, Xianda Guo, Tian Yang, Junjie Huang, Jiankang Deng, Guan Huang, Dalong Du, Jiwen Lu, and Jie Zhou. Gait recognition in the wild: A benchmark. In *Proceedings of the IEEE/CVF International Conference on Computer Vision (ICCV)*, pages 14789–14799, 2021. [2](#), [5](#), [6](#)
- [107] Shinan Zou, Chao Fan, Jianbo Xiong, Chuanfu Shen, Shiqi Yu, and Jin Tang. Cross-covariate gait recognition: A benchmark. In *Proceedings of the AAAI Conference on Artificial Intelligence (AAAI)*, pages 7855–7863, 2024. [2](#), [5](#), [6](#), [7](#)

Silhouette-based Gait Foundation Model

Supplementary Material

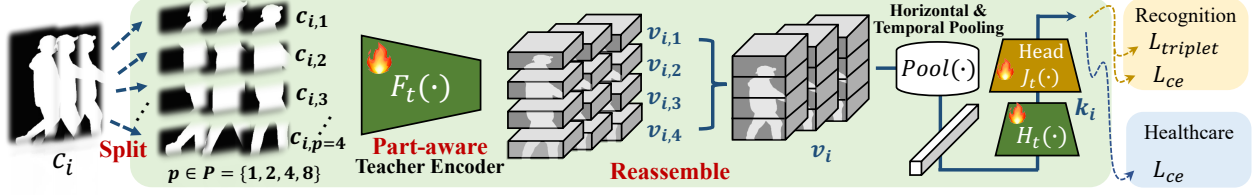


Figure 5. **Overview of Fine-tuning.** The model is initialized from pretrained teacher weights, replacing its predictor with a new task-specific head (in yellow) and keeping the part-aware training strategy active.

6. Supplementart Material

This supplementary material provides additional details on the downstream finetuning procedure of FoundationGait and the experiment settings of the ablation section.

6.1. Downstream Fine-tuning

Pipeline. To adapt the pretrained FoundationGait to downstream tasks, we apply three modifications, summarized in Fig. 5. First, following DINOv2 [53], we fine-tune the teacher model, as it provides more stable and expressive features than the student counterpart. Second, to maintain fine-grained part-level diversity, the part-aware training mechanism used in pretraining is kept active during finetuning. This preserves local structural cues in the learned representations and prevents feature homogenization. Finally, following GaitSSB [12], we replace the pretrained predictor with a randomly initialized task-specific head (J_t), paired with the appropriate objective functions for each task.

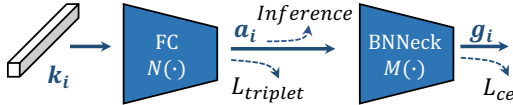


Figure 6. Recognition Head during Fine-tuning.

Recognition Head. As illustrated in Fig. 6, the recognition head takes the projector output k_i as input. It first maps k_i to an identity embedding a_i through a linear fully connected (FC) block, which is subsequently refined by a BNNeck block—a BatchNorm layer followed by a linear layer—to enhance discriminability. Two losses are applied: a triplet loss ($\mathcal{L}_{triplet}$) that enforces metric separation, and a cross-entropy loss (\mathcal{L}_{ce}) for identity classification. Their formulations are listed below:

$$\mathcal{L}_{triplet} = \sum_i [\|a_i - a_i^+\|_2^2 - \|a_i - a_i^-\|_2^2 + m]_+, \quad (4)$$

where a_i , a_i^+ , and a_i^- denote the anchor, positive, and negative embeddings, respectively, and m is the margin.

$$\mathcal{L}_{ce} = - \sum_i \log p(y_i | g_i), \quad (5)$$

where $p(y_i | g_i)$ is the predicted probability of the ground-truth identity label y_i .

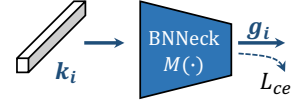


Figure 7. Healthcare Head during Fine-tuning.

Healthcare Head. Unlike the recognition task, healthcare prediction is purely a classification problem. Therefore, no FC block is used, and the BNNeck block directly outputs the category logits, as illustrated in Fig. 7. The loss follows the same formulation as Eq. 5, with the identity label replaced by the corresponding category label.

6.2. Ablation Settings

This section provides the experimental details for Sec. 4.6.

Part-aware Effectiveness. All models are pretrained on WebGait-2M in a self-supervised manner. Except for the part-aware hyperparameter P , all remaining implementation details follow Sec. 4.2. For fair comparison, we also adopt the part-aware strategy for both cropping and masking, instead of using random region operations.

Extension in Supervised Models. We scale up DeepGaitV2 to 0.03B / 0.13B using the settings in Tab. 2. The part-aware hyperparameter $P = [1, 2, 4, 8]$, and other supervised training details follow the OpenGait [13] codebase.

ViT Replacement. All models are pretrained on WebGait-2M. All implementation details follow Sec. 4.2.

Cross-modality Generalization. For the parsing-based FoundationGait, we directly replace the silhouette with the $1 \times 64 \times 44$ parsing input during fine-tuning. All other training details follow Sec. 4.4. For the parsing+sil. variant, we use a simple result-fusion scheme: during evaluation, the metric distances from the parsing and silhouette models are directly averaged. Unlike existing multimodal methods, this approach doesn't require a dedicated, complex fusion module and is straightforward to apply.

7. Human Subjects and Ethical Considerations

All experiments use publicly available gait datasets collected with informed subject consent. We strictly adhere to their original licenses and usage policies to ensure full protection of subject privacy.